Int. J. Electrochem. Sci., 16 **(2021)** Article Number: 211047, doi: 10.20964/2021.10.21

International Journal of
ELECTROCHEMICAL
SCIENCE
www.electrochemsci.org

Preparation of Keggin-type Polyoxomolybdate and its Application as Electrochemical Sensor for Detection of Levodopa

Miao Liu[†], *Mingxuan Jia*[†], *Yifeng E, Zhuozhe Li and Donghui Li*[*]

Pharmaceutical College, Jinzhou Medical University, Jinzhou, 121001, P.R.China
[†]Miao Liu and Mingxuan Jia contributed equally to this work.
[*]E-mail: lidonghuilx@sina.com

Received: 18 June 2021 / *Accepted:* 3 August 2021 / *Published:* 10 September 2021

In this study, a levodopa (LDA) electrochemical sensor based on Keggin-type polyoxometalate was constructed. First, the silicomolybdenum heteropoly acid $SiMo_{12}$ imidazole was synthesized by hydrothermal method. Fourier transform infrared absorption spectrometry (FTIR), X-ray diffraction (XRD), scanning electron microscopy (SEM) and atomic force microscopy (AFM) were used to characterize the synthetic material. Then the $SiMo_{12}$ imidazole was dropped onto the surface of a glassy carbon electrode (GCE) to construct an electrochemical sensor for detecting LDA. The sensing interface of the modified electrode was studied by cyclic voltammetry (CV) and electrochemical impedance spectroscopy (EIS). Under the optimal experimental conditions, the constructed electrochemical sensor had good detection performance for LDA with a linear range of 1×10^{-7} mol/L ~ 8×10^{-6} mol/L and a limit of detection (LOD) of 0.48×10^{-7} mol/L. Satisfactory results were also obtained in the detection of LDA tablets.

Keywords: Keggin-type polyoxomolybdate; Levodopa; Electrochemical detection

1. INTRODUCTION

Levodopa (LDA) is the metabolic precursor of catecholamine hormones, neurotransmitters and melanin in organisms. As one of the most effective drugs for the treatment of Parkinson's disease, LDA has been used for more than 30 years and is still irreplaceable [1-3]. In addition to treating Parkinson's disease, LDA can also be used to treat diseases such as dope-responsive dystonia, hepatic encephalopathy, amblyopia, restless legs syndrome and schizophrenia [4,5]. As a dopamine drug that can enter the central nervous system, LDA itself has unique advantages, and the development of compound preparations that improve its bioavailability in the body that has occurred in recent decades

has further developed the application of LDA in the neurological and spiritual fields [6,7]. However, long-term use of LDA in the human body may cause many adverse reactions, such as gastrointestinal symptoms and cardiovascular symptoms [8,9]. Therefore, to reduce the toxicity and side effects of LDA on the human body and achieve better curative effects, it is necessary to monitor and control the content of LDA in body fluids and pharmaceutical preparations.

At present, the main methods for detecting LDA include visible-ultraviolet spectrophotometry [10,11], thin layer chromatography (TLC) [12,13], high performance liquid chromatography (HPLC) [14,15], capillary electrophoresis [16,17], flow injection analysis (FIA) [18,19], and high-performance liquid chromatography coupled with mass spectrometry (HPLC–MS) [20]. However, these methods often require expensive equipment and long detection times, and some methods require complicated pretreatment processes for the samples. In contrast, electrochemical sensors have the advantages of low cost, high sensitivity, rapid detection and easy operation, which have great potential for application to the detection of LDA. However, bare electrodes often exhibit a low rate of electron transfer to LDA. Fortunately, some nanomaterials can serve as electrode modification materials and can significantly improve the selectivity and sensitivity of electrodes [21-23]. Teixeira et al. constructed a carbon paste electrode modified with a trinuclear ruthenium ammine complex $[(NH_3)_5Ru^{III}–O–Ru^{IV}(NH_3)_4–O–Ru^{III}(NH_3)_5]^{6+}$(Ru-red) incorporated into NaY zeolite for detecting LDA, and the proposed electrochemical sensor could achieve the sensitive detection of LDA. In addition, the results of testing this method on LDA tablets were consistent with those of the established method [24]. Yaghoubian et al. used carbon paste electrode modified with ferrocene (FC) and carbon nanotubes to detect LDA, and under optimized conditions, the constructed sensor could achieve sensitive detection of LDA in urine [25]. Leite et al. adsorbed chloro(pyridine)bis(dimethylglyoximato)cobalt(III) ($Co(DMG)_2ClPy$) on multi-walled carbon nanotubes and made a base-plane pyrolytic graphite electrode for the detection of LDA, and the constructed modified electrode was successfully applied to the sensitive detection of LDA in pharmaceutical preparations. [26]. In order to improve the sensitivity of electrochemical sensors, researchers have made much effort in the field of nanomaterials, and some new materials such as polyoxometalates, organic frameworks, and nanocomposite materials have been introduced into the assembly of electrochemical sensors [27-30].

Polyoxomolybdates (POMs) are a class of compounds composed of metals (such as niobium, tantalum, and tungsten) and oxygen. These compounds are mainly composed of $\{MO_6\}$ octahedrons and $\{MO_4\}$ tetrahedrons as the basic building units, and are connected by co-angle, co-edge or co-planar structures [31]. POMs have various sizes, adjustable multifunctional structures, rich composition and reversible redox properties, giving them potential application value in catalysis and materials [32,33]. At present, electrochemical sensors based on POMs have been applied in many situations. For example, Liu et al. constructed an electrochemical biosensor for detecting uric acid based on Dawson structure-based POMs, under optimized conditions, the sensor had good analytical performance for uric acid [34]. Xin et al. prepared a POM-modified electrode that could be used for highly sensitive detection of heavy metal chromium ions, and it also showed good detection performance in actual water samples [35]. Therefore, it is of great significance to develop an electrochemical sensor based on POMs for rapid and sensitive detection of LDA.

In this study, Keggin-type polyoxymolybdate ($SiMo_{12}$ imidazole) was used as the electrode modification material and fixed on the surface of the glassy carbon electrode by Nafion dispersion to prepare an electrochemical sensor for detecting LDA. The electrochemical performance of the modified electrode was studied by CV and EIS methods, and the sensitive detection of LDA was realized by differential pulse voltammetry (DPV). The constructed electrochemical sensor based on polyoxometalates can be used for the sensitive detection of LDA in pharmaceutical preparations (tablets), and has great application potential in the detection of drugs in vivo and in vitro.

2 EXPERIMENTAL

2.1 Materials

2.2.1 Reagents

In this study, through previously published method, $SiMo_{12}$ imidazole was synthesized by rotating heating [36]. LDA (purity ≥ 99.0%) was provided by Shanghai Macleans Biochemical Technology Co., Ltd., and stored in a refrigerator at 4 ℃. Levodopa tablets (250 mg/tablet) were purchased from Shanghai Fuda Pharmaceutical Co., Ltd.. N,N-Dimethylformamide (purity ≥ 99.5%) was provided by Tianjin Guangfu Technology Co., Ltd.. In addition, Nafion solution (5 wt%) was obtained from DuPont, USA. $Na_2SiO_3·9H_2O$, $Na_2MoO_4·2H_2O$ and imidazole (purity ≥ 99.0%) were all sourced from Shanghai Macleans Biochemical Technology Co., Ltd.. Hydrochloric acid and ethanol (analytical purity) were provided by Tianjin Tianli Chemical Reagent Co., Ltd. All solutions were made with pure water.

2.2.2 Apparatus

A magnetic stirrer was used to synthesize $SiMo_{12}$ imidazole (*SMI*), which was from Aika Instrument Equipment Co., Ltd. (Guangzhou, China). In addition, *SMI* was analyzed by FTIR-920 Fourier transform infrared spectrometer (Tianjin Tianguang Optical Instrument Co., Ltd.). The electrochemical behavior of different electrodes was characterized by on a CHI660E electrochemical analysis workstation (Shanghai Chenhua Instrument Co., Ltd.). The morphology of *SMI* was observed by using a scanning electron microscope (FEI NOVA NanoSEM230, USA) and an AFM-6800 atomic force microscope (Suzhou Feishman Precision Instrument Co., Ltd.). A TDM-10 X-ray diffractometer (Dantong Tongda Technology Co., Ltd.) was used to characterize *SMI*.

2.2 Methods

2.2.1 Synthesis of SMI

SMI was synthesized according to the literature [36]. In this procedure, 6.80 g $Na_2SiO_3·9H_2O$ and 0.4840 g $Na_2MoO_4·2H_2O$ were dissolved in 200 mL of water, and then the pH of the solution was adjusted to between 1 and 3 with 4 mol/L HCl. The prepared solution was continuously stirred at 90 ℃ for 30 min. Then 0.68 g of imidazole was added into the solution, and the solution was stirred

continuously at 90 ℃ for 2 h. The solution was concentrated to 100 mL and cooled to room temperature. The powdered crystals were collected to obtain *SMI*.

2.2.2 Preparation of the GCE/SMI/Nafion sensor

The specific process of preparing the sensor is shown in Scheme 1. The glassy carbon electrode was polished with 1.0, 0.3, and 0.05 μm Al_2O_3 powder on a chamois before use, and then the electrode was cleaned with distilled water and methanol in an ultrasonic cleaner. The bare electrode was dried with nitrogen. Then, 0.02 g of *SMI* was dissolved in 25 mL of N,N-dimethylformamide and ground thoroughly in a mortar until a clear yellow-green solution was formed. The GCE/*SMI* electrode was made by dropping 10 μL of the above solution on the surface of the glassy carbon electrode and drying it at room temperature for 8 h. In addition, 10 μL of Nafion dispersion was simultaneously added to the surface of the GCE/*SMI* electrode to obtain the GCE/*SMI*/Nafion electrode, which was dried in the dark at room temperature for later use. According to published literature [37,38], it can be inferred that the electrochemical reaction of LDA on the surface of the sensor obeyed the Nernst equation for a two electron and proton transfer reaction, and the reaction equation is shown in Scheme 2.

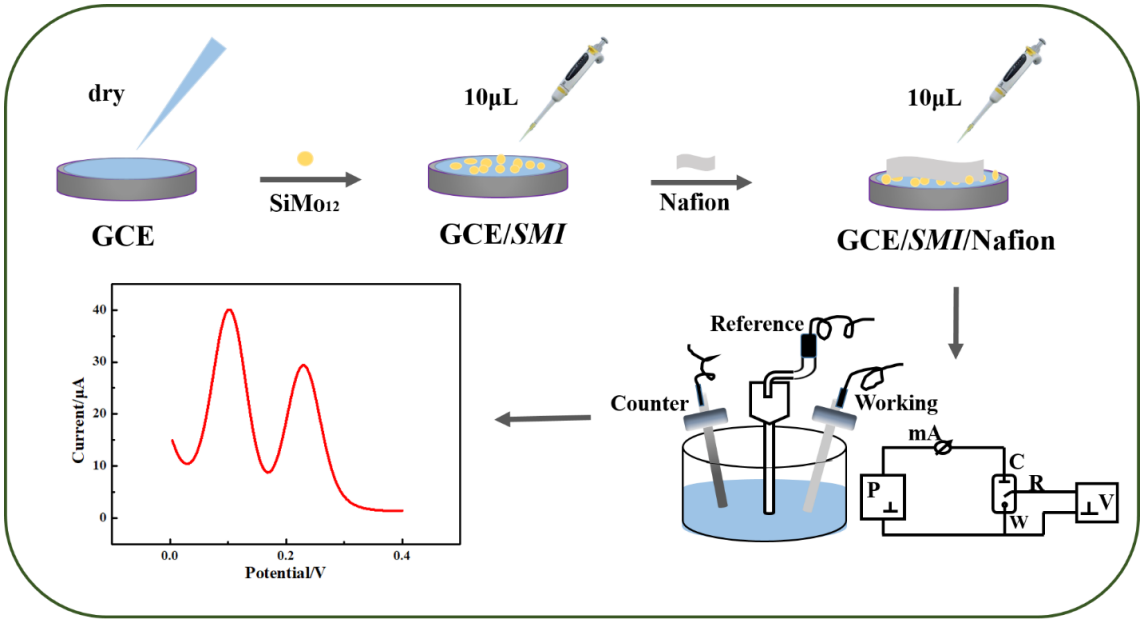

Scheme 1 Schematic diagram of the manufacturing process of the sensor and the reaction of LDA on the sensor

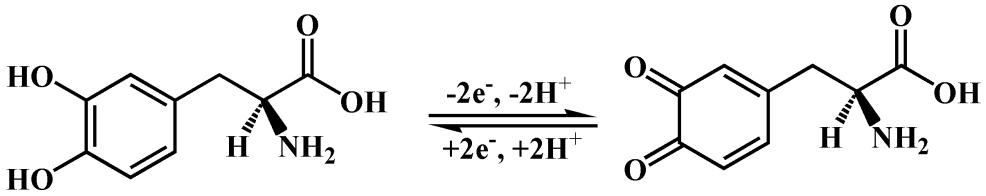

Scheme 2 Redox reaction of LDA on GCE/*SMI*/Nafion sensor

2.2.3 Experimental preprocessing

Before the experiment, the 0.1% Nafion solution was made by diluting 0.5% Nafion solution with ethanol. Next, 0.0197 g of LDA tablets was dissolved in 100 mL of HCl at a concentration of 0.1 mol/L, and after a series of filtration operations, LDA sample solutions with different concentration gradients were obtained. A stable CV curve was obtained in the scan range of 0 V ~ 0.4 V with a scan rate of 100 mV/s, and quantitative analysis of the drugs was carried out using DPV in 0.1 mol/L HCl a the scan rate of 100 mV/s. It is worth mentioning that the detection of LDA was carried out in a dark environment, and all the experiments were carried out at room temperature.

3 RESULTS AND DISCUSSION

3.1 Characterization of SMI

3.1.1 IR spectrogram

IR spectroscopy is a method that uses the characteristic wavenumber of chemical bonds to identify compounds, and it can be used to study the structure and chemical bonds of molecules. In this experiment, a Fourier transform infrared spectrometer was used to confirm the synthesis of *SMI*. As shown in Figure 1, 1092 cm^{-1} is the vibration peak of Si-O, the peaks at 957 cm^{-1} and 906 cm^{-1} are related to the asymmetric vibration and symmetric vibration peaks of Mo = O_t, and the symmetrical and non-symmetrical vibration peaks of Mo = $O_{\mu/v}$ are 957 cm^{-1} and 906 cm^{-1}, respectively. The absorption peak positions of the symmetrical vibration are 796 cm^{-1} and 865 cm^{-1}. These results are consistent with the literature [36,39], which indicates that the synthesized material has the basic structure of Keggin-type polyoxomolybdate.

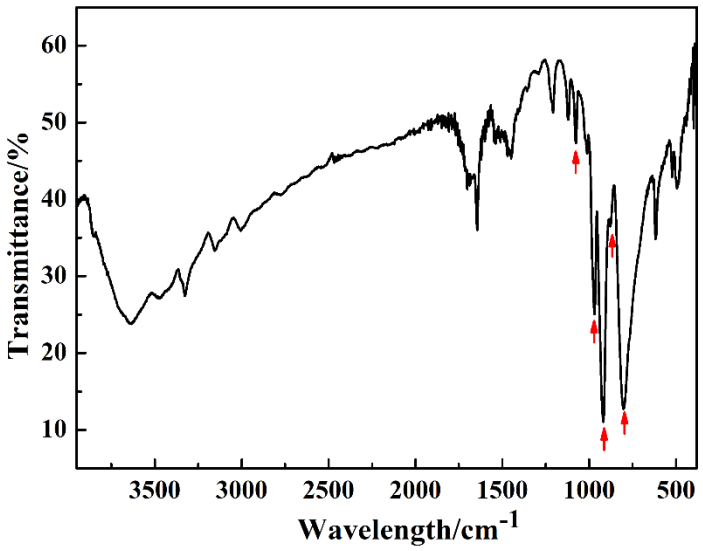

Figure 1 Infrared spectrum of *SMI*

3.1.2 XRD spectra of SMI

To further verify *SMI*, X-ray diffraction (XRD) was used to characterize the crystal lattice of *SMI*. Figure 2 shows the diffraction peaks with a diffraction angle 2θ in the range of 7~38°, corresponding to the characteristic peaks of *SMI*, which is consistent with reference [40]. These results indicated the successful preparation of *SMI*.

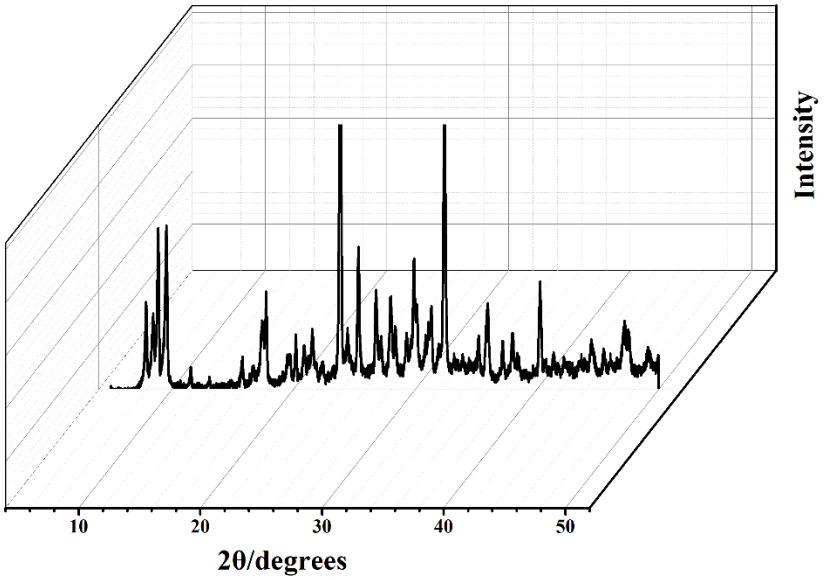

Figure 2 XRD spectrum of *SMI*

3.1.3 AFM and *SEM images of SMI*

The surface morphology of *SMI* was studied by atomic force microscopy (AFM). Figure 3A and Figure 3B show the two-dimensional and three-dimensional structures of *SMI*, respectively. The AFM images exhibited uniform size and good dispersion of *SMI*. A scanning electron microscope (SEM) is an instrument that can test the surface morphology of the sample. It uses high-energy electron beam to scan the sample. Through the interaction between the beam and the material, the purpose of characterizing the microscopic morphology of the material is achieved. To further illustrate the surface morphology of *SMI*, scanning electron microscopy (SEM) was employed in this work. As shown in Figure 4, the compound has fine particles, a rectangular shape, uniform particle size, and good dispersibility, and the particle size distribution is consistent with that shown in the AFM image, the particle size can form lead to the formation of a stable and uniform sensing interface in an electrochemical sensor.

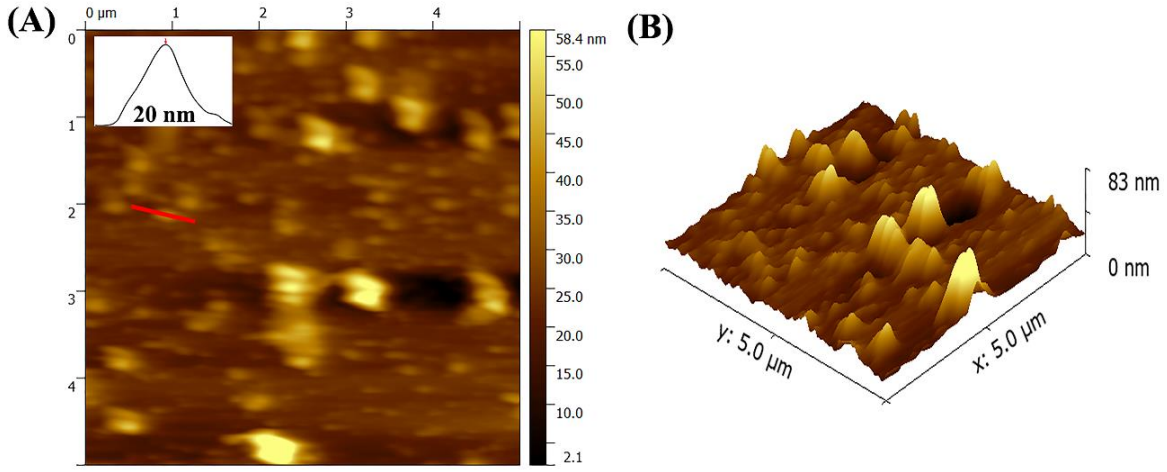

Figure 3 (A) Two-dimensional AFM image of *SMI*; (B) Three-dimensional AFM image of *SMI*

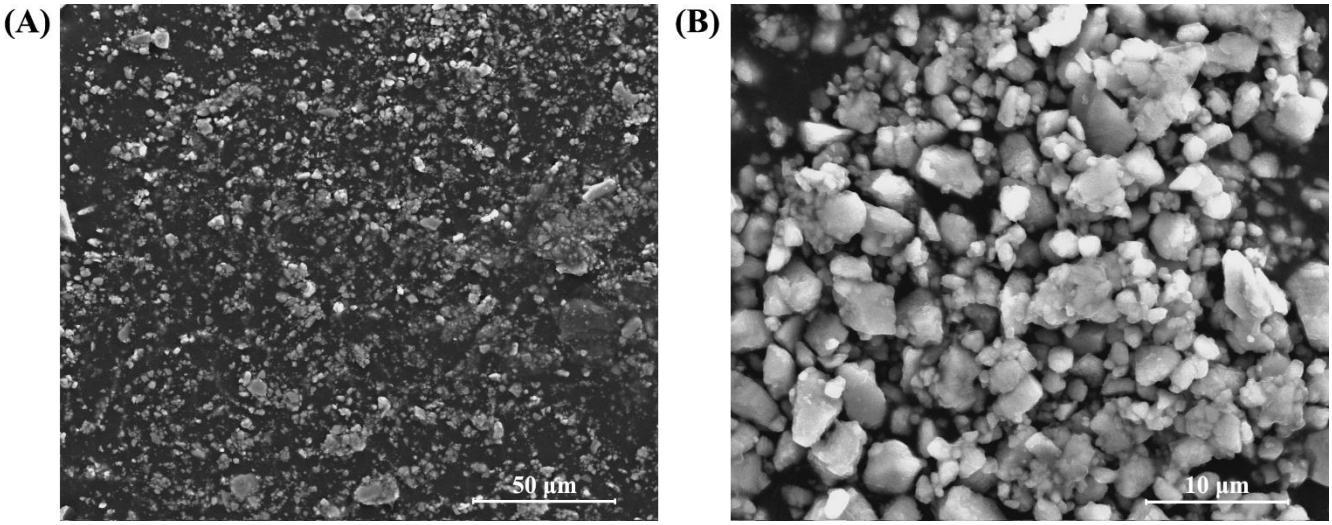

Figure 4 SEM images of *SMI* in different scales

3.2 Electrochemical characterization of electrode

3.2.1 Electrochemical behavior of the sensors

Figure 5A shows the CV graph of the bare electrode and GCE/*SMI*/Nafion modified electrode in 0.1 mol/L HCl. The bare electrode has almost no redox peak in HCl, and the peak current is difficult to observe. However, the GCE/SMI/Nafion modified electrode has two pairs of redox peaks, and the peak current values are significantly higher than that of the bare electrode, this peak may be the characteristic peak of polyoxymolybdate *SMI*. The above results show that the modified material has characteristic peak currents at 0-0.4V and a high electron transfer rate, which is beneficial to further experiments. Figure 5B shows the electrochemical impedance spectra (EIS) of the bare glassy carbon electrode and the GCE/*SMI*/Nafion electrode in 0.1 mol/L HCl. The inset shows the Randles equivalent circuit for

fitting the Nyquist plot [41-42], the axis intercept in the low frequency region represents the intrinsic impedance, the diameter of the semicircle represents the charge transfer impedance, the diameter of the semicircle in the impedance spectrum reflects the current change of the electrode [43]. It can be seen from the figure that the impedance value R_{ct} of the bare glassy carbon electrode is 2000 Ω, while the impedance value R_{ct} of the GCE/SMI/Nafion modified electrode is 200 Ω, which indicates that the introduction of *SMI* can significantly improve the conductivity of the sensing interface, and it also indicates the successful modification of *SMI* on the bare glassy carbon electrode.

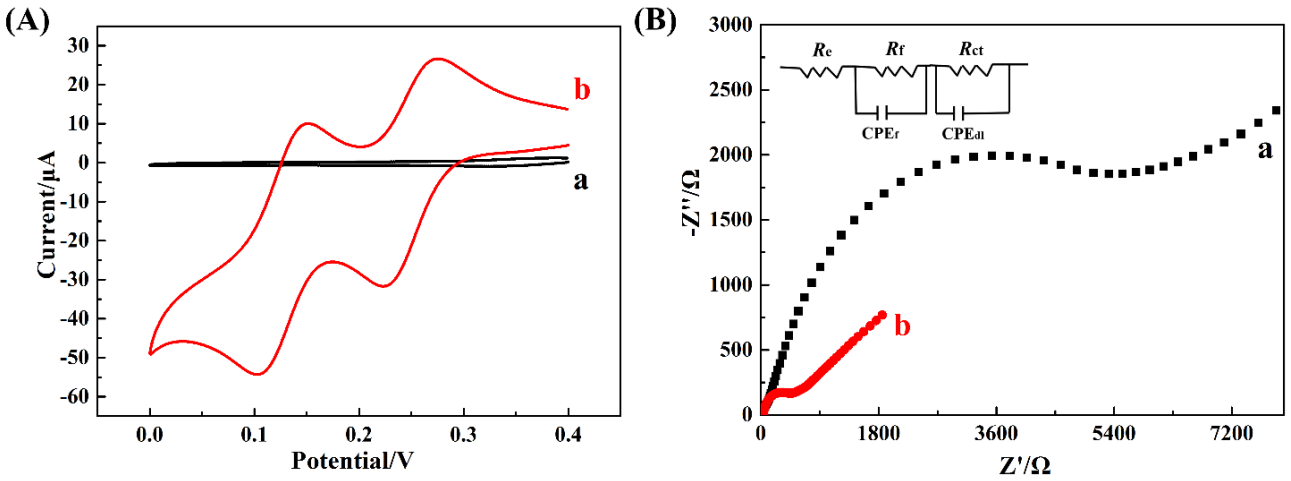

Figure 5 (A) CV characterization of the bare electrode (a) and GCE/*SMI*/Nafion modified electrode (b) in 0.1 mol/L HCl solution at a scan rate of 100 mV/s. (B) EIS characterization of the bare electrode (a) and GCE/*SMI*/Nafion modified electrode (b) in 0.1 mol/L HCl solution.

3.2.2 Optimization of experimental conditions

To obtain excellent detection performance of the electrochemical sensor for LDA, the amount of *SMI* and pH of the electrolyte were optimized in this study.

Different modified amounts of *SMI* can significantly affect the peak current intensity of the electrochemical sensor. As shown in Figure 6A, the peak current of the modified electrode increased with increasing *SMI*. When the amount of *SMI* was 0.02 g, the peak current reached a maximum, while when the amount of *SMI* exceeded 0.02 g, the peak current decreased accordingly. This trend may be because the *SMI* concentration on the electrode surface was too high, causing a reduction in the area of the electrode surface in contact with the electrolyte, thereby prolonging the activation time of the sensor. However, an excessively too high amount of *SMI* hindered the electron transfer of the modified electrode and cause the peak current to decrease. Therefore, the optimal amount of *SMI* was determined to be 0.02 g.

The pH of the electrolyte can also affect the detection performance of the electrochemical sensor to a certain extent. The three-electrode system was placed in electrolytes of different acidity, and the peak current values were collected on the modified electrode. As shown in Figure 6B, in the pH range of 1~7, the peak current decreased with increasing pH, indicating that the modifier more easily promoted

electron transfer of the sensor under acidic conditions. Therefore, pH=1 was chosen as the best detection condition.

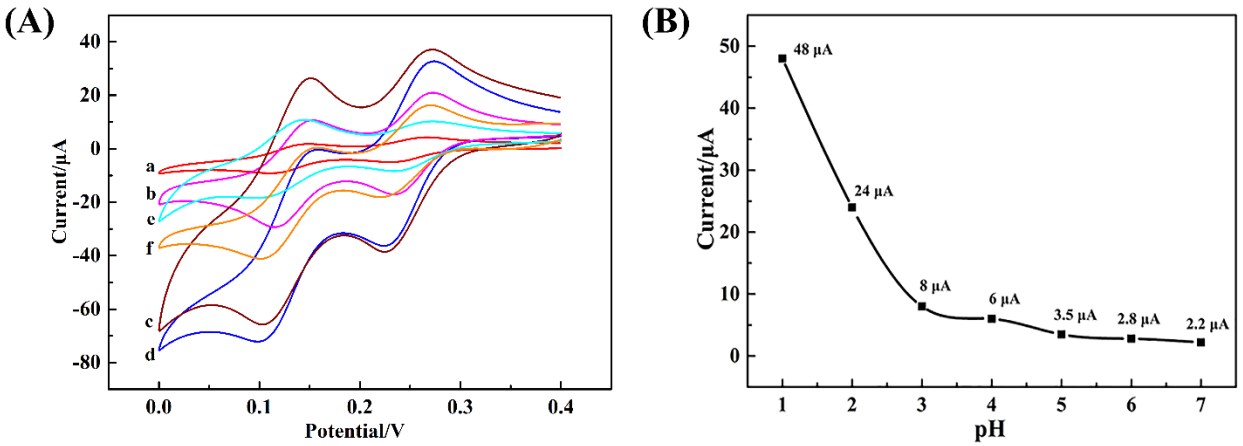

Figure 6 (A) CV current responses of the sensor with various concentrations (a: 0.0050 g, b: 0.01 g, c: 0.02 g, d: 0.03 g, e: 0.04 g, f: 0.05 g) of *SMI*; (B) Optimization of electrolyte pH (pH=1, 2, 3, 4, 5, 6, 7)

3.2.3 Study of scanning rate

The influence of scan rate on the peak current of GCE/*SMI*/Nafion modified electrode was studied by CV [44]. Figure 7A shows the CV of peak current and different scan rates with the GCE/*SMI*/Nafion modified electrode in the voltage range of 0~0.4 V and in 1×10^{-4} mol/L LDA solution (scan rates: 20, 40, 60, 80, 100, 120 , 140, 160, 180, 200 mV/s). The oxidation peak and reduction peak marked in the figure are fitted. Figure 7B shows that the scan rate is in the range of 20 ~ 200 mV/s, and the value of the modified electrode oxidation peak current (I_{pa}) is in good agreement with the scan rate. The linear relationship can be expressed as I_{pa} = 0.1744 ν + 24.23 (R^2=0.9779), the slope is 10.1744; the value of the reduction peak current (I_{pc}) conforms to the equation: I_{pc}= -0.3286 ν - 37.106 (R^2=0.9889), and the slope is -0.3286. We also studied the linear relationship between the value of the peak current and the square root of the scan rate (Figure 7C). The linear equation is I_{pa}= 3.4020 $\nu^{1/2}$ + 9.2373 (R^2=0.9976); I_{pc}= -0.6353 $\nu^{1/2}$ - 9.4218 (R^2=0.9994). Figure 7D shows the linear relationship between the logarithm of the value of the peak current and the logarithm of the scan rate. The linear equation is I_{pa}= 0.386 log ν + 0.866 (R^2=0.9993), and the slope is 0.386; the other linear equation is I_{pc}= -0.42 log ν - 1.025 (R^2=0.9986), and the slope is -0.42. Based on the following equations [45]:

$$E_{pa} = E^{0'} + m\left[0.78 + \ln\left(D^{1/2}{k_s}^{-1}\right) - 0.5\ln m\right] + \frac{m}{2}\ln v$$

$$m = \frac{\mathrm{RT}}{(1-\alpha)nF}$$

$$E_{pc} = E^{0'} + m'\left[0.78 + \ln\left(D^{1/2}{k_s}^{-1}\right) - 0.5\ln m'\right] - \frac{m'}{2}\ln v$$

$$m' = \frac{\mathrm{RT}}{\alpha nF}$$

$$\log k_s = \alpha\log(1-\alpha) + (1-\alpha)\log\alpha - \log\frac{RT}{nFv} - \frac{(1-\alpha)\alpha F\Delta E_p}{2.3RT}$$

Preliminary calculation of rate constant (*ks*) through electrochemical parameters, showed that the GCE/*SMI*/Nafion modified electrode had faster electron transfer when detecting LDA, and the constructed electrochemical sensor was controlled by diffusion throughout the process [46].

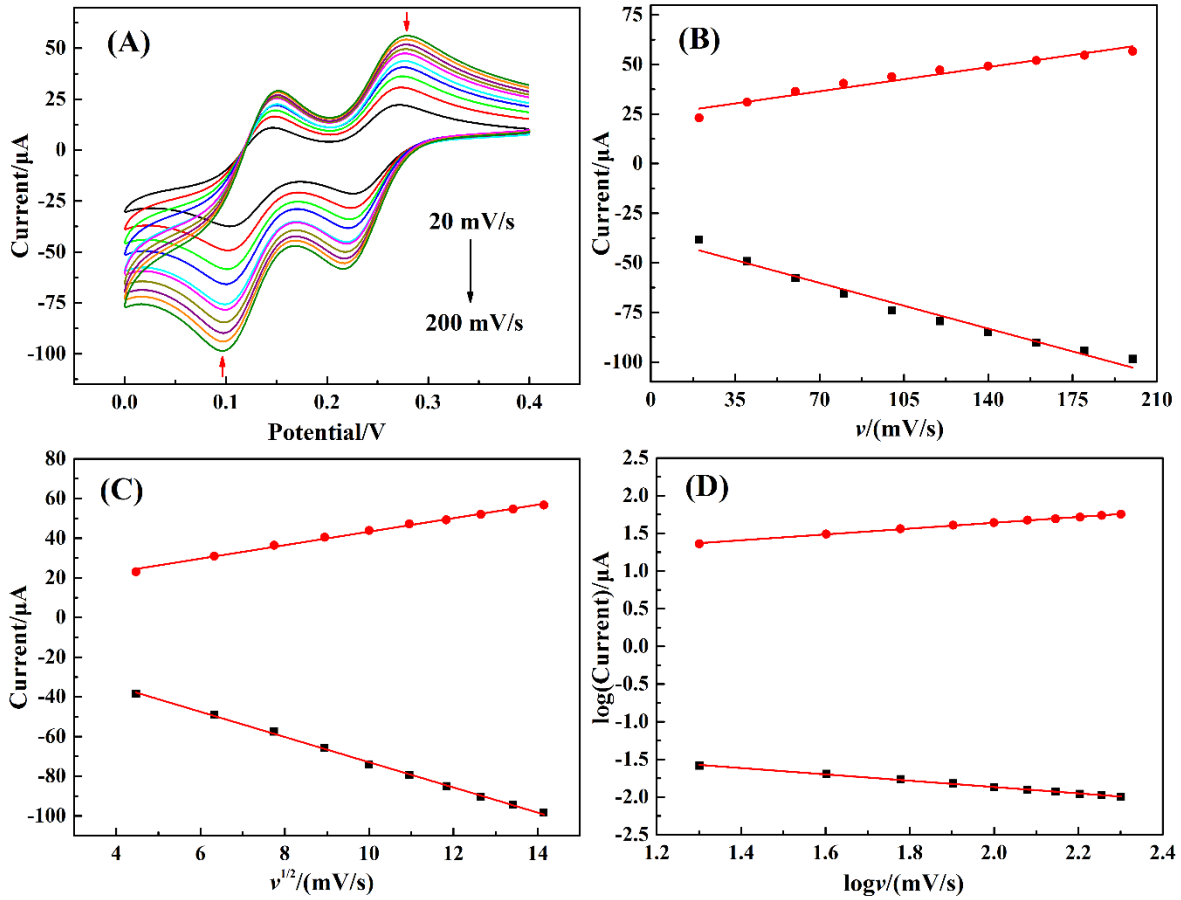

Figure 7 (A) CVs of GCE/*SMI*/Nafion tested in 1×10^{-4} mol/L LDA solution at different scan rates; (B) The relationship between the reduction peak current and the scan rate; (C) The relationship between the reduction peak current and the square root of the scan rate; (D) The relationship between the log of the reduction peak current and the log of the scan rate.

3.2.4 Determination of LDA by GCE/SMI/Nafion sensor

Under optimized experimental conditions, DPV was used to detect different concentrations of LDA. As shown in Figure 8, the oxidation peak currents (shown by the arrow) have a good linear relationship with different concentrations of LDA, and its linear range is 1.0×10^{-7} mol/L ~ 8.0×10^{-6} mol/L, The linear equation can be expressed as I_p = 54.8378 + 0. 3756 *c* (R^2=0.9976). According to the formula L=3.3*S_b/S [47], the detection limit of this method is 0.48×10^{-7} mol/L (S/N=3).

Table 1 shows a comparison between several detection methods and this method. Compared with high-performance liquid chromatography and liquid chromatography-mass spectrometry, the constructed electrochemical sensor has a lower detection limit, does not require a complicated sample processing, and it has a low detection cost. Compared with other electrochemical detection technologies,

this method does not require a complicated electrode modification process, and also has excellent detection performance. To a certain extent, it can become an ideal method for detecting LDA.

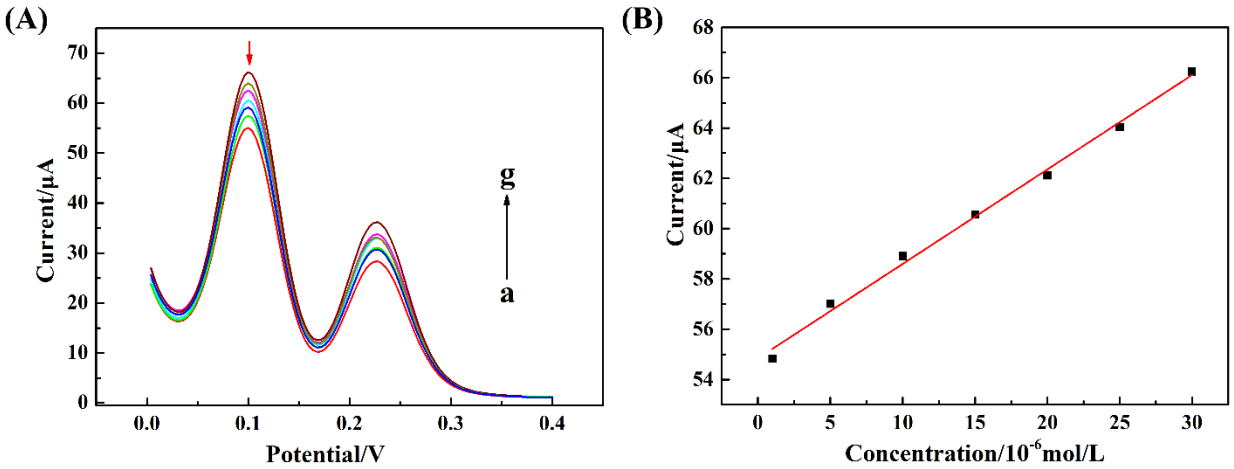

Figure 8 (A) DPV graphs of GCE/*SMI*/Nafion in solutions containing different concentrations of LDA; (B) Graphs of the relationship between redox peak current and LDA concentration

Table 1 Comparison with other methods of detecting LDA

Method	Linear range	LOD	Reference
High-performance liquid chromatography	0.05-2 μg/mL	10 ng/mL	[48]
Liquid chromatography coupled with mass spectrometry	50-5000 ng/mL	50 ng/mL	[49]
Ferrocene modified carbon paste electrode	2-500 μmol/L	1.2 μmol/L	[25]
Fe_3O_4@SiO_2/MWCNT film modified electrode	10-600 μmol/L	2 μmol/L	[50]
Poly(4-methyl-ortho-phenylenediamine)/MWNT modified GC electrode	0.416-400 μmol/L	0.1 μmol/L	[51]
Carbon nanotubes within a poly(allylamine hydrochloride) film modified electrode	2-27 μmol/L	0.84 μmol/L	[52]
Iron oxide nanoparticle and multiwalled carbon nanotube modified electrodes	0.1-8 μmol/L	0.2 μmol/L	[53]

Graphite nanoplatelets and gold nanoparticles modified electrode	5-50 μmol/L	0.5 μmol/L	[54]
Gold screen-printed electrode	1-660 μmol/L	0.99 μmol/L	[55]
Polyoxomolybdate modified electrode	0.1-8 μmol/L	0.048 μmol/L	This work

3.2.5 Reproducible and stability

The reproducibility of the GCE/*SMI*/Nafion modified electrode was investigated by using the same electrode to test 2×10^{-5} mol/L LDA for 10 consecutive times, and the relative standard deviation (RSD) of the 10 test results was 3.28%, indicating that the constructed sensor has good reproducibility. The stability of the modified electrode was also examined by using CV. After 200 continuous scans, the RSD of the peak current was 2.19%, indicating that the GCE/*SMI*/Nafion modified electrode was stable.

3.2.6 Detection of actual samples

To assess the practicability of the constructed electrochemical sensor, solutions of LDA tablets at different concentrations were tested by using the newly-proposed strategy. 0.0197 g of levodopa tablet powder was dissolved into 100 mL of HCl with a concentration of 0.1 mol/L to obtain sample solutions of levodopa with different concentrations, and the standard addition method was utilized to determine the contents of LDA. As shown in Table 2, the LDA recovery rate measured by the GCE/*SMI*/Nafion modified electrode was between 97.8% and 103.4%, and the RSD of each sample was less than 5%, indicating that the modified electrode can be used for the detection of actual samples.

Table 2. Determination of GCE/*SMI*/Nafion electrode recovery (n=5)

Sample	Initial/(mol/L)	Add/(mol/L)	Detect/(mol/L)	Recovery/%	RSD/%
1	5.00	5.00	10.34±0.23	103.4	2.12
2	10.00	5.00	14.86±0.20	99.1	1.82
3	15.00	5.00	19.56±0.13	97.8	0.89

4. CONCLUSION

In this work, an electrochemical sensor based on Keggin-type polyoxymolybdate was constructed for the sensitive detection of LDA in pharmaceutical preparations. The sensor makes full use of the special properties of polyoxymolybdate, combined with the film-forming properties of Nafion aqueous solution, so that the stability and electron transfer rate of the modified electrode are significantly improved. In view of the above advantages, the new Keggin-type polyoxymolybdate-based electrochemical sensor has achieved wide linearity and high sensitivity in the detection of LDA, and it has shown great potential in the ultra-sensitive monitoring of small molecule targets. In addition, the

feasibility of this method was confirmed by analyzing LDA in actual samples, which provides a new practical platform for drug analysis and clinical diagnosis.

ACKNOWLEDGMENTS
This work was supported by the Liaoning Provincial Department of Education Fund Project (JYTJCZR 2020082).

References

1. P.A. LeWitt, *Mov Disord*., 30 (2015) 64.
2. O. Hornykiewicz, *J Neurol*, 257 (2010) 249.
3. J.G. Nutt, *Mov. Disord.*, 23 (2008) S580.
4. S. Wijemanne and J. Jankovic, *Nat Rev Neurol.*, 11 (2015) 414.
5. R.A. Hauser, *Eur Neurol.*, 62 (2009) 1.
6. M. Yoosefian, E. Rahmanifar and N. Etminan, *Artif Cells Nanomed Biotechnol*, 46 (2018) 434.
7. J. Goole and K. Amighi, *Int J Pharmaceut.*, 380 (2009) 1.
8. R. Vasta, A. Nicoletti, G. Mostile, V. Dibilio, G. Sciacca, D. Contrafatto, C. E. Cicero, L. Raciti, A. Luca and M, Zappia, *PLoSONE*, 12 (2017) e0172145.
9. M. Ogawa, Y. Zhou, R. Tsuji, J. Kasahara and S. Goto, *Front. Neurol*, 10 (2019) 1258.
10. M. Blanco, J. Coello, H. Iturriaga, S. Maspoch and N. Villegas, *Anal Lett*, 33 (2000) 2701.
11. N. Tajodini, A. Moghimi and K. Karimnezhad, *J Adv Pharm Edu Res.*, 10 (2020) 153.
12. I. A. Sima, D. Casoni and C. Sârbu, *J Liq Chromatogr R T.*, 36 (2013) 2395.
13. S. Mohapatra, P. Ganguly, R. Singh and C. K. Katiyar, *J AOAC Int.*, 103 (2020) 678.
14. F. Elbarbry, V. Nguyen, A. Mirka, H. Zwickey and R. Rosenbaum, *Biomed. Chromatogr.*, 33 (2019) e4382.
15. V. B. Subramanian, N. Konduru, N.K. Katari, T. Dongala and R. Gundla, *Sep Sci plus.*, 3 (2020) 530.
16. A.M. Zeid, J.J.M. Nasr, F.F. Belal, S. Kitagawa, N. KAJI, Y. BABA and M.I. Walash, *RSC Adv.*, 6 (2016) 17519.
17. P.T.T. Ha, A.V. Schepdael, T. Hauta-aho, E. Roets and J. Hoogmartens, *Electrophoresis*, 23 (2002) 3404.
18. L.H. Marcolino-Júnior, M.F.S Teixeira, A.V. Pereira and O. Fatibello-Filho, *J Pharmaceut Biomed*, 25 (2001) 393.
19. Y. Zhang and S.Y. Gao, *Adv Mat Res.*, 884 (2014) 566.
20. K. V. Özdokur, E. Engin, Ç. Yengin, H. Ertaş and F.N. Ertaş, *Anal Lett.*, 51 (2018) 73.
21. N.J. Yang, G.M. Swain and X. Jiang, *Electroanalysis*, 28 (2016) 27.
22. S. Alim, J. Vejayan, M.M. Yusoff and A.K.M. Kafi, *Biosens. Bioelectron.*, 121 (2018) 125.
23. C.Z. Zhu, D. Du, A. Eychmüller and Y.H. Lin, *Chem. Rev.*, 115 (2015) 8896.
24. M.F.S. Teixeira, M.F. Bergamini, C.M.P. Marques and N. Bocchi, *Talanta*, 63 (2004) 1083.
25. H. Yaghoubian, H. Karimi-Maleh, M.A. Khalilzadeh and F. Karimi, *Int. J. Electrochem. Sci.*, 4 (2009) 993.
26. F.R.F. Leite, C.M. Maroneze, A.B. de Oliveira, W.T.P dos Santos, F.S. Damos and R. de C. S. Luz, *Bioelectrochemistry*, 86 (2012) 22.
27. M. Liu, M.X. Jia and D.H. Li, *Int. J. Electrochem. Sci.*, 15 (2020) 10141.
28. S. Carrasco, *Biosensors*, 8 (2018) 92.
29. Y.H. Xiao and C.M. Li, *Electroanalysis*, 20 (2008) 648.
30. S. Shrivastava, N. Jadon and R. Jain, *Trends Analyt Chem.*, 82 (2016) 55.

31. D. Wang, L.L. Liu, J. Jiang, L.J. Chen and J.W. Zhao, *Nanoscale*, 12 (2020) 5705.
32. T. Ueda, *ChemElectroChem*, 5 (2018) 823.
33. M. Ramezani-Aliakbari, A. Soltanabadi, H. Sadeghi-aliabadi, J. Varshosaz, B. Yadollahi, F. Hassanzadeh and M. Rostami, *J. Mol. Struct.*, 1240 (2021) 130612.
34. C. Liu, M.Q. Xu, Z.L. Tan, S. Li, Y. Wang, Y.L. Wang and J.Q. Sha, Z. *Anorg. Allg. Chem.*, 646 (2020) 489.
35. X. Xin, N. Hu, Y.Y. Ma, Y.L. Wang, L. Hou, H. Zhang and Z. Han, *Dalton Trans.*, 49 (2020) 4570.
36. C.-D. Wu, C.-Z. Lu, S.-M. Chen, H.-H. Zhuang and J.-S. Huang, *Polyhedron*, 22 (2003) 3091.
37. X Guo, H. Yue, S. Huang, X. Gao, H. Chen, P. Wu, T. Zhang and Z. Wang. *J. Mater. Sci.-Mater. Electron.*, 31 (2020) 13680.
38. Y. Wang, H. Zhang, M. Chen. *Anal. Chim. Acta*., 1157 (2021) 338379.
39. H. Wang, Y.-P. Chen, Z.-C. You, M.-X. Zhou, N. Zhang and Y.-Q. Sun, *Chin. Chem. Lett.*, 26 (2015) 187.
40. Y. Zhao, F. Li, Z. Sun, Y. Zhang and L. Xu, *Inor Chem Commun*, 70 (2016) 83.
41. M. Fingar, K. Xhanari and B. Petovar. *Microchem J.*, 147 (2019) 863.
42. K. Jian, L. ZF and W. Guannan. *Bioelectrochemistry*, 137 (2020) 107647.
43. K.Y. Goud，A. Hayat，G. Catanante，M. Satyanarayana，K.V. Gobi and J.L. Marty. *Electrochim. Acta*, 244 (2017) 96.
44. S.U. Karabiberoglu and Z. Dursun, *J. Electroanal. Chem.*, 815 (2018) 76.
45. S. Wei, Y. Wang, Y. Zhang, X. Ju and Z. Sun. *Anal. Chim. Acta*, 751 (2012) 59.
46. H. Lv, Y. Li, X. Zhang, Z. Gao, J. Feng, P. Wang and Y. Dong. *Anal. Chim. Acta*., 1007 (2018) 61.
47. G.L. Long and J.D. Winefordner. *Anal. Chem.*, 55 (1983) 712A.
48. I. Baranowska and J. Plonka. *J. Chromatogr. Sci.*, 1 (2008) 30.
49. I.C. César, R.M.D. Byrro, F. Fernandes de S.S. Cardoso, I.M. Mundim, L.S. Teixeira, S.A. Gomes, R.R. Bonfima and G.A. Pianetti. *J. Mass. Spectrom.*, 46 (2011) 943.
50. M.R. Ganjali, H. Salimi, S. Tajik., H. Beitollahi, M. Rezapour and B. Larijani. *Int. J. Electrochem. Sci.*, 12 (2017) 5243.
51. M.A. Kamyabi and N. Rahmanian. *Anal. Methods*, 7 (2015) 1339.
52. H.H. Takeda, T.A. Silva, B.C Janegitz, F.C. Vicentini, L.H.C. Mattoso and O. Fatibello-Filho. *Anal. Methods*, 8 (2016) 1274.
53. V.Baiao, L.I.N. Tome and C.M.A. Brett. *Electroanalysis*, 30 (2018) 1.
54. T.R. Silva, A. Smaniotto and I.C. Vieira. *J. Solid State Electrochem.*, 22 (2018) 1277.
55. M.F. Bergamini, A.L. Santos, N.R. Stradiotto and M.V.B. Zanoni. *J Pharmaceut. Biomed.*, 39 (2005) 54.